Ensemble modeling of very small ZnO nanoparticles†

Franziska Niederdraenk,[a] Knud Seufert,[a] Andreas Stahl,[a] Rohini S. Bhalerao-Panajkar,[bc] Sonali Marathe,[b] Sulabha K. Kulkarni,[d] Reinhard B. Neder[e] and Christian Kumpf*[af]

Received 1st June 2010, Accepted 7th October 2010
DOI: 10.1039/c0cp00758g

The detailed structural characterization of nanoparticles is a very important issue since it enables a precise understanding of their electronic, optical and magnetic properties. Here we introduce a new method for modeling the structure of very small particles by means of powder X-ray diffraction. Using thioglycerol-capped ZnO nanoparticles with a diameter of less than 3 nm as an example we demonstrate that our ensemble modeling method is superior to standard XRD methods like, *e.g.*, Rietveld refinement. Besides fundamental properties (size, anisotropic shape and atomic structure) more sophisticated properties like imperfections in the lattice, a size distribution as well as strain and relaxation effects in the particles and—in particular—at their surface (surface relaxation effects) can be obtained. Ensemble properties, *i.e.*, distributions of the particle size and other properties, can also be investigated which makes this method superior to imaging techniques like (high resolution) transmission electron microscopy or atomic force microscopy, in particular for very small nanoparticles. For the particles under study an excellent agreement of calculated and experimental X-ray diffraction patterns could be obtained with an ensemble of anisotropic polyhedral particles of three dominant sizes, wurtzite structure and a significant relaxation of Zn atoms close to the surface.

Introduction

Nanoparticles and clusters with sizes below 5–10 nm represent an exceptional case since their properties can neither be described by classical solid state physics nor by molecular physics. Even when crystalline particles often have a structure similar to the bulk structure, they cannot be considered just as small bulk crystals since their reduced size has major consequences: obviously, the ratio between surface and bulk atoms is drastically increased and thus surface effects play an important role. The surface cannot be neglected any more, as it is done in many solid state approaches. Furthermore, when the particles' size falls below characteristic length scales of solid state physics, quantum confinement effects arise and become dominant. An exciton, *e.g.*, is confined when its Bohr radius reaches the order of the physical dimension of the particle. The nanoparticle is then called "quantum dot". One effect caused by the small size is an increase of the bandgap with all its consequences for the electronic and optical properties of the particle. Hence, changing the size of nanoparticles allows us to continuously tune these properties, which is the origin for a variety of applications.[1–5]

The particle size is the key quantity in this context. However, more dedicated parameters like shape, structure, strain, disorder, *etc.* also play an important role when the particle properties shall be understood in detail. Therefore, the investigation of such properties has attracted more and more attention recently. Several studies demonstrated that chemical, optical, and electronic properties are more strongly influenced by these attributes than it was assumed earlier.[6–8] Furthermore, it can be crucial to distinguish between size, shape, and surface effects, especially for applications which need well-defined samples. For this reason, an accurate size determination as well as a detailed analysis of the nanoparticle structure is of great importance.

A very common method for the size determination of nanoparticles is UV/Vis spectroscopy. With the help of effective mass or tight binding models the size dependent change of the band gap is used to obtain the particle size from optical absorption spectra (excitonic excitations). However, since these theoretical models are based on solid state or molecular approaches and adapted for nano-sized materials, they give only rough approximations of the real dimensions of the crystallites. Furthermore, other effects like the particle shape, defects or strain are neglected but can nevertheless influence the optical properties significantly. Another much more costly technique for nanoparticle characterization is high-resolution transmission electron microscopy (HRTEM). This method offers much more information than UV/Vis spectroscopy. Since it is a local probe, only a very small number of particles

[a] *Physikalisches Institut der Universität Würzburg (EP2), D-97074 Würzburg, Germany*
[b] *DST Unit on Nanoscience, Department of Physics, University of Pune, Pune-411007, India*
[c] *Department of Engineering & Applied Sciences, VIIT, Pune-411048, India*
[d] *Indian Institute of Science Education & Research, Pune-411021, India*
[e] *Lehrstuhl für Kristallographie und Strukturphysik, Universität Erlangen, D-91058 Erlangen, Germany*
[f] *Institute of Bio- and Nanosystems (IBN-3), Research Center Jülich, and JARA-Fundamentals of Future Information Technologies, 52425 Jülich, Germany. E-mail: c.kumpf@fz-juelich.de*

† Electronic supplementary information (ESI) available: Details and fitting parameters for Rietveld and ensemble modeling. See DOI: 10.1039/c0cp00758g

(usually not more than 100) can be investigated. Hence, this method is limited when average parameters for an ensemble of particles shall be investigated. This often represents a disadvantage, even though detailed parameters of individual particles like defects or stacking faults can be observed. Another aspect which should not be overlooked is the fact that mostly the larger or only the largest particles of a sample are analyzed since it is much easier to find them in the ensemble of particles and obtain images with sufficiently good contrast. This is the reason for HRTEM tending to overestimate the average crystallite size for samples that consist of differently sized particles.

An alternative method which is frequently applied for the analysis of nanoparticles is powder X-ray diffraction. It provides valuable information about the size and structure, if the measurement and the analysis of the data are carefully performed. The most common way of analyzing powder diffraction patterns is a Rietveld refinement. This yields the widths of the Bragg peaks from which the average particle size can be calculated using the Scherrer equation. A homogeneous particle structure must be assumed for the Rietveld method in order to fit the Bragg reflections. Thus, the method works well for nanoparticles having a well ordered structure similar to the corresponding bulk structure. Depending on the material this is the case for particles larger than $\sim$5 nm in diameter. Below this size (and therefore for the most interesting particles), the assumption breaks down, especially if the nanoparticles exhibit crystalline defects or surface strain since these effects cannot be taken into account by the Rietveld method. The same holds for parameter distributions like a size distribution of the particles in the sample. In general, modern Rietveld programs usually yield a very good fit to the experimental data. However, often this is due to the big number of artificial parameters which are implemented in the code (like, *e.g.*, asymmetric and θ-dependent line shapes) but the interpretation of them can be very difficult.

To overcome these limitations, we have developed an ensemble modeling method, which is able to consider all structural parameters mentioned above, in particular, size distributions, different shapes, defects like stacking faults and (surface) strain. Since a nanoparticle model is generated atom by atom in this method, in principle any structural feature can be realized. Unlike the Rietveld refinement, the modeling technique intrinsically involves all particle parameters and thus much more information is directly available.

In this paper we present this new method by means of one exemplary data set obtained from ZnO nanoparticles with an excitonic diameter of about 5.6 nm. This material was chosen since it is one of the most prominent prototypes for nanoparticles and has been studied already very well with a variety of experimental methods. It is also used in many applications.[9–11] In a detailed comparison with the results of a Rietveld refinement and a step by step analysis we demonstrate that very fine structural details can be determined with our ensemble modeling method.

The method is of general applicability to any nano-system which can be investigated by means of (powder) X-ray diffraction, in particular to free-standing nanoparticles and clusters. The approach is unique in its capability of accessing ensemble-properties and in its richness of structural details which can be obtained with very high precision. Similar approaches for the analysis of diffraction patterns are rare. To our knowledge, the only examples to be found in literature are Bawendi *et al.*[12] and Murray *et al.*[13] In both publications CdS, CdSe and/or CdTe nanoparticles are investigated using relatively simple particle shapes like spheres or ellipsoids. Bawendi *et al.* included structural imperfections to some extent and Murray *et al.* additionally considered a small size variation around a fixed average value which was determined by TEM. However, a more realistic size distribution, a systematic investigation of particle shapes, or a more sophisticated consideration of the effects of surface relaxation, defects or imperfections were not implemented in their modeling.

Experimental

Synthesis

The nanoparticles presented here were wet-chemically synthesized. Solutions of NaOH and $ZnCl_2$ in methanol are mixed to form small ZnO nanocrystals in a precipitation reaction. Thioglycerol serves as stabilizing agent, which allows us to control the size of the crystallites by varying the concentration and simultaneously preventing an agglomeration. After washing and drying, the nanoparticles are available as a powder. For details of the synthesis see Ashtaputre *et al.*[14]

Powder X-ray diffraction

The XRD data were taken using the *z*-axis diffractometer at the wiggler beamline BW2 of the Hamburger Synchrotronstrahlungslabor (HASYLAB). This enabled reasonable scattering intensities and limited data acquisition times. However, the method does not depend on the use of Synchrotron Radiation. The photon energy in the experiment was 9600 eV (λ = 1.292 Å), well below the Zn 1s absorption edge. Since the width of Bragg reflections from very small nanoparticles can reach values close to those of amorphous materials and therefore typically show low peak intensity, a special experimental setup was chosen for the measurements. In order to reduce parasitic scattering from amorphous and polycrystalline materials in the beam paths the nanoparticle powder was drop-coated onto a silicon single crystal wafer and carefully oriented in the X-ray beam in such a way that scattering from the Si wafer was avoided. Additionally, beam paths and sample chamber were helium flooded during the measurement so that air scattering could be suppressed. θ–2θ-scans in a range from $2\theta \approx 1$–90° were performed, corresponding to a scattering vector $q = 4\pi \sin(\theta)/\lambda \approx 0.1$–$7.5$ Å^{-1}. Instead of one long scan several identical fast scans were taken in order to detect (and consequently avoid) beam damage in the sample. The individual scans were summed up and analyzed with the method described below.

Data analysis with Rietveld refinement

For a Rietveld refinement[15–17] a certain crystalline structure must be assumed which defines the parameters that can be adjusted in the fit. From this structure the positions of the Bragg reflections are calculated. The finite widths of the

individual peaks are described by convolution with a peak profile function. Often also a small asymmetry for the reflections is allowed. Furthermore lattice parameters and the position of the oxygen atom in the unit cell are refined. The background is usually adjusted by a polynomial. Imperfectness can at best be considered by a mixture of particles having different structures. However, in a Rietveld refinement each individual particle is assumed to be perfectly ordered. Here we used and compared two different Rietveld codes, SIMREF[16] and FULLPROF,[17] both with wurtzite as the fundamental crystalline structure for ZnO. The reflections were fitted with a pseudo-Voigt profile having a slightly asymmetric line shape. When using the FULLPROF code individual line widths were allowed for all reflections in order to obtain information about an asymmetric particle shape. For the background a polynomial of fifth order is used.

Data analysis with ensemble modeling

The refinement *via* ensemble modeling is based on the computer simulation of an ensemble of individual atomic models of the nanoparticles and the calculation of the corresponding diffraction intensity *via* the Debye equation:[18,19]

$$I(q) = \sum f_j^2 + \sum f_i f_j \frac{\sin(qr_{ij})}{qr_{ij}},$$

where f_i and f_j are the atomic form factors, and r_{ij} the length of the interatomic vector between atoms i and j. Internally, the program uses a faster algorithm for the calculation, which was developed by Hall *et al.*[20] and Cervellino *et al.*[21] The atomic coordinates for an individual particle are generated from a small set of structural parameters such as lattice parameters, particle diameter, defect parameters *etc*., for details see below. The refinement of these structural parameters is carried out using an evolutionary algorithm.[22]

The simulation of defect free nanoparticles is made by expanding the unit cell to a suitably large crystal that is then cut to the required size and shape by removing atoms outside a sphere or set of lattice planes. Such a nanoparticle may contain a few tens or up to several thousand atoms. As for the Rietveld refinement, the structure is built up according to only a few parameters which determine the atomic positions in one asymmetric section of a single unit cell. The only additional parameters required are those defining the shape of the particle.

In several situations the simulation of the nanoparticles is modified. This is, *e.g*., the case when stacking faults shall be considered. A nanoparticle is then simulated by stacking atomic layers on top of each other according to a growth fault model.[23] Mixed structures of wurtzite (stacking sequence ABAB) and zincblende structures (AB′CAB′C) can be simulated easily following this method.‡ The probability for the next layer being of a certain type is determined by a weighted random choice. Since the nanoparticles are small, typically 5 to 50 layers, they will contain only a small number of stacking faults. However, the structure of each individual particle depends on the exact location of the stacking faults in the particle and therefore the diffraction pattern will slightly differ from particle to particle even though all fit parameters (including the stacking fault probability) are identical. Hence, an ensemble of particles must be simulated by averaging the diffraction pattern of several (typically $\sim$50) individual nanoparticles. The final diffraction pattern is then compared to the experimental data.

Size distributions, *i.e*., a mixture of particles with different sizes, can also be considered by the ensemble averaging. This effect can be realized by two different approaches. In the first approach, many individual nanoparticles are simulated with individual randomly chosen radii. The probability for a given radius is determined according to a size distribution function. In the second approach, a few nanoparticles are simulated with several fixed radii. Their individual diffraction intensities are weighted according to a size distribution function. In the case of the ZnO nanoparticles in this study it turned out that the second approach is sufficient for an adequate description.

The structural parameters that are typically refined in this work include lattice parameters, atomic positions in the asymmetric unit, atomic displacement parameters, defect parameters such as stacking fault probabilities or strain parameters, and particle size parameters. The latter parameters easily allow the simulation of anisotropic particle shapes and size distributions. Furthermore, we also included the consideration of surface relaxation effects by allowing the position of surface near atoms to vary from their ''bulk-'' like position. The refinement of these structural parameters is carried out *via* a variant of the evolutionary algorithm.[22] This kind of algorithm is chosen since the simulation involves the average of several diffraction patterns, which have been calculated from individual nanoparticles using random defects. It represents a very reliable method for finding the global minimum in parameter space. On the other hand, it makes the simulations quite time-consuming. Depending on the size of the modeled nanocrystals and whether or not ensembles have to be considered (due to stacking faults or a size distribution), the required time to refine a model varies from several hours to weeks. For judging the quality of the fit we used the weighted R-value:

$$R_{\mathrm{wp}} = \sqrt{\frac{\sum_j w_j \left(I_{\mathrm{obs},j} - I_{\mathrm{calc},j}\right)^2}{\sum_j w_j I_{\mathrm{obs},j}^2}},$$

where w_j is the weighting, $I_{\mathrm{obs},j}$ and $I_{\mathrm{calc},j}$ are observed and calculated intensities, respectively, for each point j of the diffraction pattern.

Results and discussion

This section is organized as follows: we initially present a comparison of the fitting results obtained by Rietveld refinement and by our new ensemble modeling method. In the second part the strategy of how to achieve a high-quality fit for a measured diffraction pattern using the ensemble modeling is illustrated.

‡ The B-layers in Wurtzite and Zincblende are not precisely identical but are mirrored with respect to each other. This difference is indicated by labeling them B and B′.

Rietveld refinement *vs.* ensemble modeling

Fig. 1 shows the comparison of two different Rietveld refinements (labelled "SIMREF" and "FULLPROF") *versus* the ensemble modeling fit. The main difference between the two Rietveld refinements is that the FULLPROF code is able to consider an anisotropic particle shape to some extent. In the case of the ensemble modeling, the best result was obtained using a nanoparticle ensemble consisting of polyhedral particles with a hexagonal basis and pure wurtzite structure. The model comprises particles of three different lateral sizes and a distorted surface. A precise description of the fitting procedure is given further below.

All three fits yield quite satisfying results. However, compared to the SIMREF fit the advantage of our modeling method is obvious. Except for minor deviations of the first double peak all reflections are extremely well reproduced, while the SIMREF fit shows several clear shortcomings: the major discrepancies are observed for *hk*0 reflections, which are much too weak, and for the *h*0l reflections, which are slightly left-shifted relative to the experimental data. Moreover, the triple peak at $q = 4.5$ Å^{-1} is overestimated in the SIMREF fit. The better overall agreement is also reflected by R_{wp} values differing almost by a factor of 2 ($R = 2.9\%$ for the ensemble modeling fit, $R = 5.4\%$ for SIMREF).

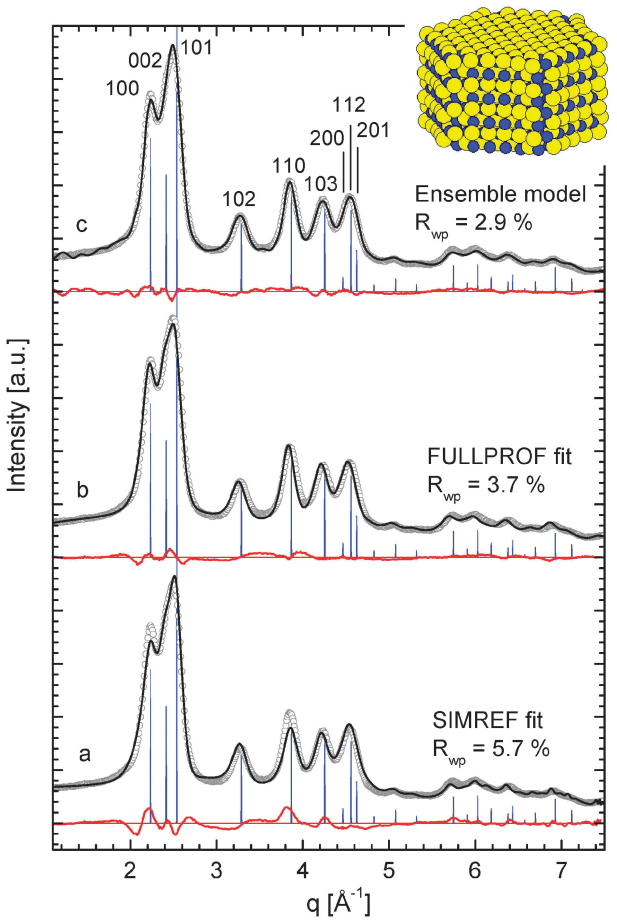

Fig. 1 Comparison of the final results of two different Rietveld refinements using (a) the SIMREF and (b) the FULLPROF code, and (c) the ensemble modeling. Open circles represent the measured data of the ZnO nanoparticles, solid lines show the diffraction patterns of the corresponding fits. The positions of ZnO bulk reflections (pure wurtzite structure) are indicated as blue lines. The inset shows the atomic arrangement of the most common nanoparticle of the ensemble represented by curve c (Zn = yellow atoms, O = blue atoms, for details see text).

As discussed above the size of the nanoparticles represents the most important parameter. Applying the Scherrer equation to the SIMREF fit-result we obtained an average particle size of 30 Å. The ensemble modeling revealed the same dominating particle size, but also (at least) two larger species (43 Å and 55 Å, for details see Table S1 provided online as ESI†).

With the FULLPROF code a fit is obtainable with similar quality as the ensemble modeling result ($R_{wp} = 3.7\%$). Basically all shortcomings of SIMREF regarding intensities are lifted, however, the peak shifts (of the 102, 110 and 103 in this case) are still visible. The good fit is a result of different peak widths for reflections of different types which are allowed in this code. They can be interpreted as different particle sizes so that an anisotropic shape of the particles can be simulated. Rod-like wurtzite particles, for example, having a larger height than width, would show narrow 00*l* and wider *hk*0 reflections. For the particles under study FULLPROF does indeed indicate an anisotropic particle shape. However, the "apparent sizes" calculated from the individual peak widths are not consistent. This can, *e.g.*, be seen for the 102 and 103 reflections which yield smaller sizes (23.3 Å and 22.3 Å, respectively) than 110 and 002 (27.0 Å and 27.4 Å, respectively). Using these particle dimensions no realistic particle can be formed. For all details see Table S2 (provided online as ESI†).

The size-anisotropy was also clearly indicated by the ensemble fitting. However, since other parameters like defects and stacking faults, which influence the coherence of the scattering process and therefore affect peak widths and intensities of individual peaks, can be considered in this modelling method, a realistic particle shape can be obtained here.

Another evident difference between the two Rietveld fits and the ensemble modeling is found for the lattice parameters. While both Rietveld fits yield unrealistically large values the results of our ensemble modeling are very close to those of the ZnO bulk. The fact that realistic lattice parameters can be obtained is a consequence of an additional sophisticated feature in our modeling: surface strain can be considered, *i.e.*, a gradient in the lattice parameter within a certain region close to the surface. Especially the position and intensity of the *h*0l reflections can be reproduced much better, when surface strain is considered. If it is neglected, too large lattice parameters partly compensate for this effect as in the case of the Rietveld refinement. Other parameters like the *z*-position of the oxygen atom in the unit cell and the atomic displacement parameter have no significant influence on the refinement. For details see Tables S1 and S2 provided online as ESI.†

In conclusion, this comparison shows that the ensemble modeling method yields a significantly better fit to the experimental data than a standard Rietveld refinement like SIMFEF. With a more sophisticated Rietveld code involving an anisotropic particle shape (FULLPROF) an almost equally good fit result can be achieved, however, no consistent particle shape can be found from the size parameters. With our

ensemble modelling method such restrictions are avoided and hence realistic shapes, distributions of parameters, *etc*. can be considered. Since real structural parameters are used as fit-parameters we have direct access to much more detailed structural information. These advantages are not gained at the expense of using a larger number of parameters. We used at max. 20 parameters, compared to 21 and 19 for the two Rietveld refinements.

Refining structural details with the ensemble modeling method

The procedure of ensemble modeling includes multiple refinement steps. In the first step, the best shape of the modeled particles is searched. Usually this is done without considering any complex features like defects, surface strain, or size distributions, which are included later. Only the dimensions of the particle, the lattice parameters and an atomic displacement parameter (ADP) are adjusted. If other information is not available, we use bulk values as corresponding starting values for lattice parameters and ADP. To obtain reasonable starting parameters for the particle size, we determine the width of some selected reflections from single-line fits of the measured data and apply the Scherrer equation. Alternatively, the results from the Rietveld refinement are used.

Different shapes. We start the modeling with the most basic shape, a spherical model. For more realistic shapes the trend of bulk crystals to form preferentially low-indexed crystallographic surfaces is anticipated and hence several different polyhedral shapes are tested. This also allows anisotropic shapes which are parameterized by several particle sizes for different crystallographic directions. Beside other effects like stacking faults or surface relaxation (see below), the anisotropic shape accounts for different peak widths which were observed in the experimental data. The results can be seen in Fig. 2, which contains calculated diffraction patterns (solid lines) for a selection of four different particle shapes (out of 10 shapes which were tested, see also ref. 24) and the corresponding measured data. The simple spherical model (curve a) features similar problems as the Rietveld refinement: the intensity of the *hk*0 reflections is much too small, while the 102, the 002/101 double- and the 200/112/201 triple peaks are overestimated.§ This imbalance is much improved by assuming a polyhedral shape. The models (b)–(d) all have one parameter for the height and (at least) one parameter for the lateral size of the particle.¶ Schematic images of all shapes can be seen in Fig. 2 as insets. The top and bottom faces of polyhedra are (001) and (00$\bar{1}$) surfaces, *i.e*., their height is just defined by the number of stacked layers. Laterally the particles have a hexagonal shape confined by six surfaces of the {100}-type. Polyhedron I (curve b) represents the symmetric version (one parameter for the lateral size) whereas polyhedron II (curve c) has a "distorted hexagon" as base face with different diameters in [100] and [010] direction (see inset in Fig. 2). The effect on the diffraction

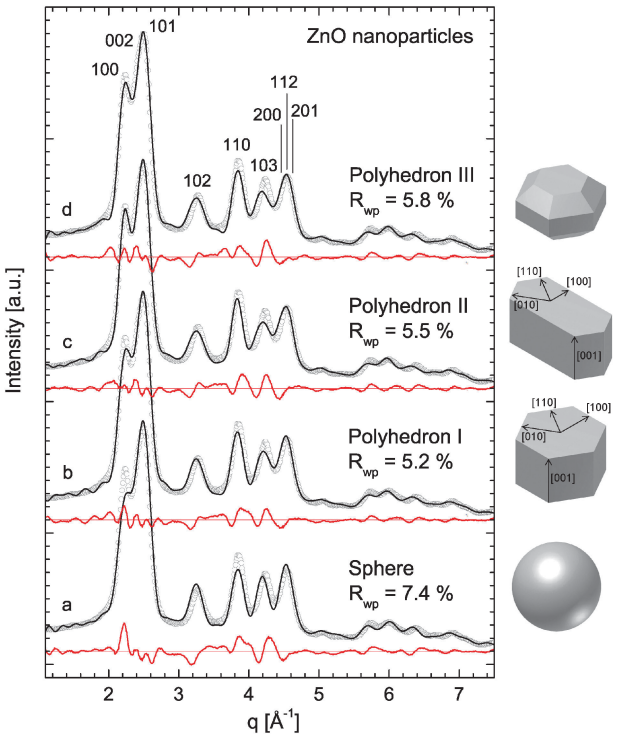

Fig. 2 Comparison of different shapes: the experimental data (open circles), calculated diffraction patterns (solid lines) and the residua are shown for four different particles shapes.

data is somewhat similar to a mixture of particles with symmetric hexagonal shape but different sizes (*i.e*., a "size distribution"). Polyhedron III has—compared to the simple case of polyhedron I—twelve additional {111}-oriented surfaces in order to prevent 90° edges at the top and at the bottom of the particle. This is parameterized by an additional (third) "diameter" in [111] direction.

The fitting of the simplest (spherical) model results in a particle diameter of 33 Å. The polyhedra, which all give a better fit to the measured data, yield anisotropic particle shapes. Several reflections of the experimental data, in particular the *hk*0 reflections, are much better reproduced by models with strong anisotropy. The height converges to about 20 Å while the lateral sizes lie between 28 and 42 Å, depending on the details of the model. All individual values are listed in Table S1 provided online as ESI.† The precise definition of particle "diameters" for the more sophisticated particle shapes can also be found there. However, clear differences in the overall fit quality among the polyhedra cannot be observed which is also indicated by rather similar *R* values (5.2% to 5.8%).

So far the results are already quite satisfying. However, there are still some discrepancies of experimental and calculated data, which indicate that the atomic models are not ideal yet. Hence we tried to improve the fit in the second step by searching for other structural features which play a role. Since none of the tested polyhedral shapes is clearly superior to the others most shape models were tested in combination with additional features.

Stacking faults. Imperfections and defects in the crystal structure are features which occur frequently in very small

§ It is consistent that the spherical model reveals the same problems as the Rietveld refinement since both are based on an isotropic particle shape.

¶ "Height" is attributed to the crystallographic [001] direction of the Wurtzite structure since this represents the direction for stacking of atomic planes.

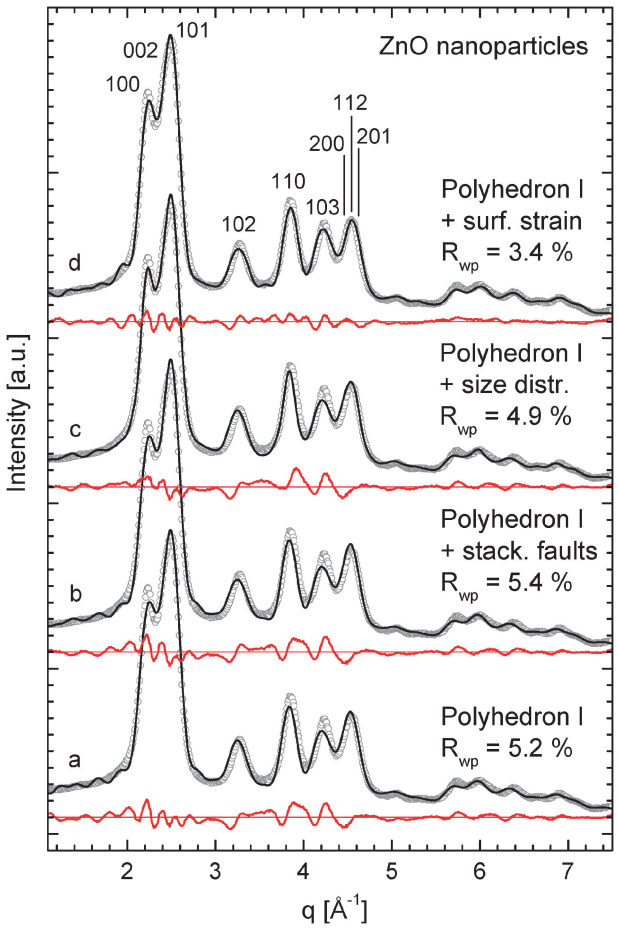

Fig. 3 Influence of further structural features: the experimental data are shown in comparison to (a) a fit based on a single particle with shape I and no defects and (b)–(d) fits with additional features. These features are (b) stacking faults, (c) a size distribution, and (d) surface strain. Note that the final fit obtained by combination of these additional features is shown in Fig. 1(c).

nanoparticles. For ZnO stacking faults are maybe the most common defects since two competing growth modes exist. Bulk ZnO has wurtzite structure, *i.e.*, it consists of layers which are stacked in the sequence ABAB... The second, competing growth mode for these crystals is AB′CAB′C..., *i.e.*, the zincblende structure. Hence, a "C"-like layer in a wurtzite structure represents a "stacking fault" in ZnO. Different layer stackings can easily be considered in the ensemble modeling method. Exemplary for all shapes this is shown by means of polyhedron I in Fig. 3a and b where the best fit resulted in a stacking fault probability of only 1.8%.

This value is negligible since, on average, it corresponds to one stacking fault for every 56th layer while one particle is composed of only 8 layers. The results for other shapes were comparable; all probabilities were below 5%. Consequently, none of the models with stacking faults could considerably improve the fitting of the experimental data. (One exception is the spherical model, where stacking faults can compensate for the lacking shape anisotropy to some extent.) This finding indicates that the ZnO nanocrystals are basically free of stacking faults, which is remarkable for very small particles. For many other samples stacking fault probabilities of up to 40% were found.[25] In the present case, however, these kind of defects can and will be neglected in all models presented in the following.

Size distribution. The refinements described in the previous sections were all based on the simulation of a single nanoparticle, *i.e.*, the "best fitting individual particle" was searched and assumed that it represents a good average for the ensemble. The fact that many structural parameters—in particular size and shape—may be subject to a distribution was neglected. Ensemble properties were limited to defects. However, a more realistic modeling of wet-chemically synthesized particles should consider at least differently sized particles. For the example discussed here, the good agreement of the "distorted hexagonal" polyhedron II with the data (in particular for the *hk*0 reflections) already gave a hint on the presence of a size distributions (see discussion above). We continued our refinement with polyhedron I, since it yielded the best fit so far, and introduced a simple implementation of a size distribution: a mixture of three different particle sizes is considered. Refinements with full degrees of freedom showed that it is sufficient to introduce different sizes for the lateral dimensions only, while the vertical size could be fixed to one common value.

The resulting fit is shown in Fig. 3c. In comparison with curve a (the same fit without size distribution) two diffraction peaks, the 100 and 110, are significantly improved. The fact that *hk*0 reflections are influenced is consistent with the introduction of additional lateral features. Even though 93% of the simulated ensemble consists of the smallest crystals with 25 Å in lateral diameter, the larger particles (40 Å and 52 Å) are essential for a high-quality fit. The particle height was refined to 24 Å for all cases.

Nevertheless, the match of the 102 and 103 reflections is still insufficient. They are shifted to lower q values and the intensity of the 103 reflection is still too weak. The shift is partly compensated for by lattice parameters, which are refined to too large values (a: +0.8%, c: +0.9% larger than the bulk values).

Surface strain. Therefore, as a last and very important step, we tried to consider the influence of the surface of the nanoparticles. The fact that the number of surface atoms reaches or exceeds the number of atoms with a bulk-like configuration in small particles of course has great influence on the structure. The most basic parameter affected by this is the lattice parameter. So far lattice parameters were assumed to be homogeneous throughout the entire particle. Now different atomic coordinations of surface and bulk atoms shall be considered by a gradual strain or relaxation in the structure. We allowed a shift of the atoms within a thin surface-near region according to a linear increase or decrease of vertical and lateral lattice parameters, separately for all atomic species.

The refinement revealed that essentially only the outermost Zn atoms of the particles are significantly displaced. This is reflected by a thickness of only 2 Å of the surface-region, a maximum outward shift for the Zn atoms of 0.44 Å in lateral

and vertical direction, and a neglectable shift of 0.02 Å for the oxygen atoms. This result can be explained by the chemistry of the particle formation. The particles are stabilized by organic ligands at their outer shell, thioglycerol in this case. With their thiol group the molecules bind to Zn atoms and limit the growth of the nanoparticles during synthesis. Our fit result indicates that only those Zn atoms which are directly bonded to the ligand molecules show relaxation. It is remarkable that, after considering the relaxation of the Zn-surface atoms only, the fit improves significantly (see Fig. 3d) even though only very few atoms are affected by the surface strain. This highlights the great importance of surface effects for a precise modeling of the structure of nanoparticles. In particular, the positions of the *h0l* reflections are much better reproduced by this model, and the overall reflection intensities are improved. This result is achieved with values for the lattice parameters, which are much closer to those of bulk ZnO. The *R* value of 3.4% quantifies the significant overall improvement for this last refinement step.

By combining the last two steps in the refinement (size distribution and surface strain) the *R*-value can even be reduced to 2.9% as can be seen in our best fit shown in Fig. 1b (see section "Rietveld refinement *vs*. ensemble modeling").

Conclusion

In conclusion, we have demonstrated that an excellent modeling of the geometric features of nanoparticles is possible with our ensemble method. It turned out to be by far superior to standard approaches like Rietveld refinement, even in the case that particle anisotropy is considered in the Rietveld code. The modeling of thioglycerol-stabilized ZnO nanoparticles was performed in four steps. First, the most fundamental parameters, the approximate size and the (anisotropic) shape of the particles, were determined. We found that, in this case, the precise shape has less influence on the diffraction pattern as long as a reasonable crystalline shape is used. In the second step the influence of lattice imperfections was tested. Since two different growth modes exist for the structure under investigation (wurtzite and zincblende), the most obvious imperfections are stacking faults. However, the fit results revealed that stacking faults do not play a significant role in these particles since on average only one stacking fault per 7 particles occurs. In contrast to the implementation of imperfections, a size distribution for the particles (step 3) and a relaxation of the surface atoms (step 4) significantly improved the fit. These two final steps were most important for achieving an excellent agreement between experimental and calculated data in the refinement. In our case an excellent *R*-value of 2.9% could be reached.

However, the strength of this new approach does not lie only in a better fit to the experimental data compared to the Rietveld approaches, but also in much more detailed information which can be obtained, including ensemble properties. Due to these additional structural details, in particular size distribution and surface strain, our method represents a significant step forward.

The final model for the ensemble of nanoparticles under study consists of stacking fault free particles with an anisotropic shape corresponding to polyhedron I (see Fig. 2). Different sizes have been identified, the smallest having a lateral size of 30 Å and a height of 24 Å. With 84% they make up the gross of the ensemble. Particles with larger sizes (43 Å/24 Å and 55 Å/24 Å in lateral diameter/height) were also identified with fractions of 4% and 12%, respectively. The particles have lattice parameters close to the bulk value but show a significant relaxation of the Zn atoms at the surface which are bonded to the stabilizing agent, the thioglycerol molecules. These Zn atoms are outwards relaxed by up to 0.44 Å.

Even though all details of this structural ensemble model are essential in order to obtain the best fit to our data, the surface relaxation plays an exceptional role since it is the only parameter which allows the fit to refine to realistic lattice parameters, *i.e.*, it removes the problem of unrealistic lattice spacings which in many cases compensates for shifted diffraction peaks. In conclusion, we demonstrated that high-quality powder X-ray diffraction in combination with sophisticated modeling methods is a very valuable tool for investigating very small nanoparticles in detail.

Acknowledgements

We thank the Volkswagen Stiftung (project I/78 909) and the Deutsche Forschungsgemeinschaft (DFG, SFB 410) for financial support. Technical assistance by the HASYLAB staff is also acknowledged. The project was supported by the IHP program "Access to Research Infrastructures" of the European Commission (HPRI-CT-1999-00040).

Notes and references

1 W. U. Huynh, J. J. Dittmer and A. P. Alivisatos, *Science*, 2002, **295**, 2425–2427.
2 V. I. Klimov, A. A. Mikhailovsky, S. Xu, A. Malko, J. A. Hollingsworth, C. A. Leatherdale, H. J. Eisler and M. G. Bawendi, *Science*, 2000, **290**, 314–317.
3 M. Bruchez, M. Moronne, P. Gin, S. Weiss and A. P. Alivisatos, *Science*, 1998, **281**(5385), 2013–2016.
4 W. C. W. Chan and S. M. Nie, *Science*, 1998, **281**(5385), 2016–2018.
5 E. B. Voura, J. K. Jaiswal, H. Mattoussi and S. M. Simon, *Nat. Med.*, 2004, **10**(9), 993–998.
6 S. Pal, B. Goswami and P. Sarkar, *J. Phys. Chem. C*, 2007, **111**, 16071–16075.
7 G. D. Scholes, *Adv. Funct. Mater.*, 2008, **18**, 1157–1172.
8 A. S. Barnard and P. Zapol, *J. Chem. Phys.*, 2004, **121**, 4276–4283.
9 C. Klingshirn, M. Grundmann, A. Hoffmann, B. Meyer and A. Waag, *Phys. J.*, 2006, **1**, 33–39.
10 Z. L. Wang, *J. Phys.: Condens. Matter*, 2004, **16**(25), R829–R858.
11 G. Rodriguez-Gattorno, P. Santiago-Jacinto, L. Rendon-Vazquez, J. Nemeth, I. Dekany and D. Diaz, *J. Phys. Chem. B*, 2003, **107**(46), 12597–12604.
12 M. G. Bawendi, A. R. Kortan, M. L. Steigerwald and L. E. Brus, *J. Chem. Phys.*, 1989, **91**, 7282–7290.
13 C. B. Murray, D. J. Norris and M. G. Bawendi, *J. Am. Chem. Soc.*, 1993, **115**, 8706–8715.
14 S. S. Ashtaputre, A. Deshpande, S. Marathe, M. E. Wankhede, J. Chimanpure, R. Pasricha, J. Urban, S. K. Haram, S. W. Gosavi and S. K. Kulkarni, *Pramana*, 2005, **65**, 615–620.
15 R. A. Young, *Introduction to the Rietveld Method*, in *The Rietveld Method*, ed. R. A. Young, Oxford University Press, Oxford, 1993, pp. 1–38.
16 C. Rebmann, H. Ritter and J. Ihringer, *Acta Crystallogr., Sect. A: Found. Crystallogr.*, 1998, **54**, 225–231.
17 J. Rodríguez-Carvajal, *Phys. B*, 1993, **192**, 55–69.

18 C. Giacovazzo, *Beyond ideal crystals*, in *Fundamentals of Crystallography*, ed. C. Giacovazzo, Oxford University Press, Oxford, 2nd edn, 2002, pp. 268–269.
19 P. Debye, *Ann. Phys*., 1915, **351**, 809.
20 B. D. Hall, M. Flueli, R. Monot and J. P. Borel, *Phys. Rev. B: Condens. Matter*, 1991, **43**(5), 3906–3917.
21 A. Cervellino, C. Giannini and A. Guagliardi, *J. Comput. Chem*., 2006, **27**, 995–1008.
22 R. Storn and K. Price, *J. Global Optim*., 1997, **11**, 341–359.
23 T. Proffen and R. B. Neder, *J. Appl. Crystallogr*., 1997, **30**, 171–175.
24 F. Niederdraenk, K. Seufert, P. Luczak, S. K. Kulkarni, C. Chory, R. B. Neder and C. Kumpf, *Phys. Status Solidi C*, 2007, **4**(9), 3234–3243.
25 R. B. Neder, V. I. Korsunskiy, C. Chory, G. Müller, A. Hofmann, S. Dembski, C. Graf and E. Rühl, *Phys. Status Solidi C*, 2007, **4**(9), 3221–3233.